PISTON
Journal of Technical Engineering:

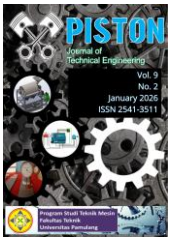

Performance Evaluation of an Integrated Heat Pump Fluidized-Bed Dryer with Solar and Biomass Furnace for Paddy Drying

M. Yahya[1], Zido Yuwazama[1,a)], Dedi Wardianto[1,b)], Putri Pratiwi[1], Delvis Agusman[2]

[1]*Department of Mechanical Engineering, Faculty of Engineering, Institut Teknologi Padang, Padang, 25173, Indonesia*
[2]*Department of Mechanical Engineering, Faculty of Industrial Technology and Informatics, Universitas Muhammadiyah Prof. DR. HAMKA, Jakarta, 12130, Indonesia*

E-mail: [a)] zidoyuwazama23@gmail.com
[b)] wardiantodedi71@gmail.com

Received: Desember 08, 2025 *Revision: Desember 15, 2025* *Accepted: Desember 31, 2025*

Abstract: This study aims to evaluate the performance of a heat pump fluidized-bed dryer incorporating a biomass furnace and a solar collector for paddy drying. The paddy moisture content (MC) was decreased from 28.52% to 16.28% on a dry basis (db) through the drying process over 23.68 minutes, under operating conditions of a mass flow rate of 0.1033 kg/s and an average temperature of 70 °C. An average drying rate of 0.042 kg/min was achieved, corresponding to a specific moisture extraction rate of 0.24 kg/kWh. Correspondingly, the system required average specific electrical and thermal energy consumptions of 7.43, 3.21, and 4.22 kWh/kg, respectively. The biomass furnace demonstrated a high thermal efficiency of 87.9%, while the solar collector achieved an average efficiency of 31.7%. The heat pump exhibited stable performance, with an average coefficient of performance measured at 3.2. The heat pump condenser, solar collector, and biomass furnace generated average heat energies of 2.37 kW, 0.79 kW, and 2.91 kW, respectively. The dryer exhibited average thermal and pickup efficiencies of 21.8% and 40.4%. The average exergy efficiency was 57.7%. Furthermore, the incorporation of the heat recovery exchanger resulted in an approximate 47% reduction in heat energy consumption.

Keywords: Paddy, Fluidized-bed Dryer, Heat Recovery, Drying, Performance.

Abstrak: *Kinerja pengering heat pump fluidized-bed yang menggabungkan kolektor surya dan tungku biomassa untuk pengeringan padi dievaluasi. Sistem pengeringan tersebut berhasil mengurangi kadar air padi dari 28,52% db menjadi 16,28% db selama 23,68 menit, pada kondisi operasi dengan laju aliran massa 0,1033 kg/s dan suhu rata-rata 70 °C. Laju pengeringan rata-rata sebesar 0,042 kg/menit tercapai, yang sesuai dengan laju ekstraksi air spesifik sebesar 0,24 kg/kWh. Dengan demikian, sistem tersebut membutuhkan konsumsi energi spesifik, listrik, dan termal rata-rata masing-masing sebesar 7,43, 3,21, dan 4,22 kWh/kg. Tungku biomassa menunjukkan efisiensi termal yang tinggi sebesar 87,9%, sedangkan kolektor surya mencapai efisiensi rata-rata sebesar 31,7%. Heat pump menunjukkan kinerja yang stabil, dengan koefisien kinerja rata-rata sebesar 3,2. Tungku biomassa, kondensor heat pump, dan kolektor surya menghasilkan energi panas rata-rata masing-masing sebesar 2,91, 2,37, dan 0,79 kW. Pengering menunjukkan efisiensi termal dan efisiensi penyerapan rata-rata masing-masing sebesar 21,8% dan 40,4%. Efisiensi eksergi rata-rata adalah 57,7%. Lebih lanjut, penggabungan heat recovery exchanger menghasilkan pengurangan konsumsi energi panas sekitar 47%.*

Kata kunci: *Padi, Fluidized-bed Dryer, Heat Recovery, Pengeringan, Kinerja.*

INTRODUCTION

As an agrarian nation, Indonesia is recognized as a major global producer of paddy rice, yielding roughly 84 million tons annually. This commodity supports the livelihoods of about 30 million Indonesian farmers [1].

Freshly harvested paddy generally exhibits elevated moisture content (MC), typically between 20% and 27% on a wet basis (wb) [2]. Under these moisture conditions, the grain is unsuitable for storage due to its increased vulnerability to microbial contamination. Consequently, the MC must be reduced to approximately 14% wb to inhibit microbial activity, minimize the risk of discoloration, and ensure its suitability for long-term storage [3].

Drying paddy is the process of decreasing the grain's moisture content by evaporating moisture through the application of heat energy to achieve a specified MC. Numerous types of drying systems are typically utilized to achieve this objective, including fluidized-bed dryers, fixed-bed dryers, open-sun dryers, rotary dryers, and inclined-bed dryers. Fluidized-bed dryers are widely adopted due to their high effectiveness compared to other drying systems. They offer several advantages, such as having a simple structural design, requiring relatively short drying times, producing high-quality dried products, and requiring low initial investment and maintenance costs. Furthermore, fluidized-bed dryers are well-suited for processing wet particulate and granular materials, including food, medicinal herbs, chemical, and agricultural and pharmaceutical [4].

The performance of a fluidized-bed dryer applied to paddy drying was investigated. The findings indicated that decreasing the paddy MC from 36.98% to 27.58% on a dry basis (db), at roughly 7.75 t/h of drying throughput and inlet air temperature of about 100–120 °C, required 7.57 and 0.79 MJ/kg of thermal and electrical energy inputs, respectively [5]. In paddy drying, a significant amount of energy is required to evaporate MC from the grains. In industrial drying applications, manufacturing operations account for nearly 12% of the total energy consumption, while the drying process represents roughly two-thirds of the overall capital investment cost [6].

Besides energy consumption, other prominent considerations for the paddy drying process include the drying rate, operational costs, type of energy source employed, and the quality of the dried grain output. At present, fossil fuels remain the primary energy source for drying processes. However, fossil-fuel reserves are limited. Additionally, they contribute to air pollution, as well as having high prices and steadily rising costs. At the same time, overall energy demand continues to increase. Solar drying offers a viable solution to fossil-fuel-based systems by utilizing solar energy to carry out the drying process. This approach offers reduced energy demand and lower operational costs relative to conventional drying systems. Moreover, solar energy is widely available in numerous regions and serves as a clean and sustainable source of power.

A variety of solar dryer designs and configurations have been introduced to process a wide range of agricultural and industrial materials. These include cabinet-type solar dryers used to dry spices and herbs [7], olive mill wastewater [8], red chili [9], and palm oil fronds [10]. Researchers have also developed other designs, such as greenhouse solar dryers [11], tunnel solar dryers [12], and dryers of Andrographis paniculata [13]. Nevertheless, their performance is constrained by low solar irradiance and intermittent sunlight, as the solar collectors are capable of capturing only a limited amount of solar energy. Solar dryers are often coupled with a biomass furnace to solve these limitations.

Integrated solar–biomass drying systems are applied to various products such as spices and medicinal herbs [14], pineapple [15], chili [16], and fish [17]. In these arrangements, the system is often described as a hot dryer where the elevated drying-air temperature increases the rate of the drying process. However, excessively high drying-air temperatures may decrease product quality. An alternative approach for enhancing the drying rate involves lowering the drying air MC, which can be achieved through dehumidification using a heat pump system.

Drying technologies integrating heat pump with biomass and solar energy sources are extensively developed for processing a wide range of products. Red chili [18], copra [19], and cassava [20] have been dried using cabinet-type solar dryers integrated with heat pump units. Also, paddy drying has been carried out using hybrid solar–fluidized-bed drying incorporating a biomass furnace and heat pump [21]. Thermal energy losses within the drying system, losses from system components, including drying chamber and the air-heating units (solar collectors, biomass burners, and biomass furnaces), serve a critical role because they raise the overall energy consumption during operation and decrease the system's energy efficiency. The integration of a heat recovery exchanger leads to reduced energy losses and enhanced drying process efficiency.

Recovery heat exchangers are implemented across various drying technologies to utilize waste heat and improve operational efficiency. Several studies have implemented this approach for different drying applications, such as cabinet solar dryers incorporating a heat-pump system for drying radish [22]; mint leaves drying using a heat pump [23]; and drying red chili using a cabinet dryer combined with a biomass furnace [24]. Fluidized-bed dryers incorporating a heat recovery exchanger with a heat pump have been evaluated. A 66.9% reduction in the energy demand for wheat drying was achieved with the implementation of a heat recovery unit [25].

Based on the existing literature, the performance of a heat pump-assisted fluidized-bed dryer incorporating a solar collector and a biomass furnace has not yet been investigated for paddy drying. Consequently, the present research focuses on the design and performance evaluation of an integrated heat pump fluidized-bed dryer incorporating a heat recovery exchanger.

METHODS

A heat pump-assisted fluidized-bed dryer incorporating a biomass furnace, a solar collector, and a heat recovery exchanger was developed and constructed. The integrated drying system comprises several major components, including solar collector, heat pump, drying chamber, blower, cyclone separator, and biomass furnace, as presented in Figure 1. A schematic of the drying system is presented in Figure 2. The biomass furnace is configured with a dedicated heat exchanger, a combustion chamber for biomass fuel oxidation, and an exhaust chimney to ensure proper flue gas discharge. The heat exchanger employed is of the cross-flow type. The biomass furnace is equipped with a two-stage heat exchanger system. The primary stage heat exchanger functions as a primary air heater, whereas the second-stage heat exchanger serves as a preheating unit as well as a heat-recovery component. A flat-plate solar collector with a single-pass flow arrangement is implemented in the system using an area of approximately 3.6 m². The heat pump system incorporates an evaporator, condenser, compressor, and capillary tube as its main components. The power input is 1 HP and the refrigerant used is R22. The evaporator and condenser are of the cross-flow fin-and-tube type. The design incorporates a drying chamber configured as a horizontal fluidized bed. The blower used to circulate the air has a power input of 3.7 kW.

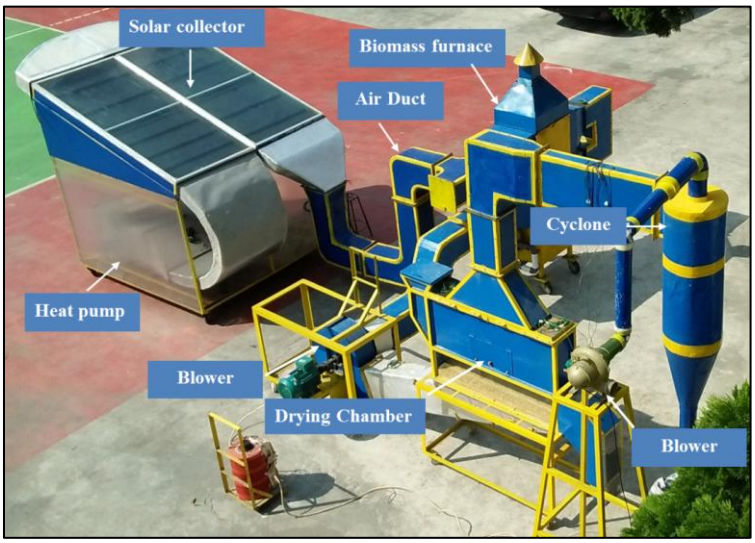

Figure 1. An integrated heat pump fluidized-bed dryer with a solar collector and a biomass furnace

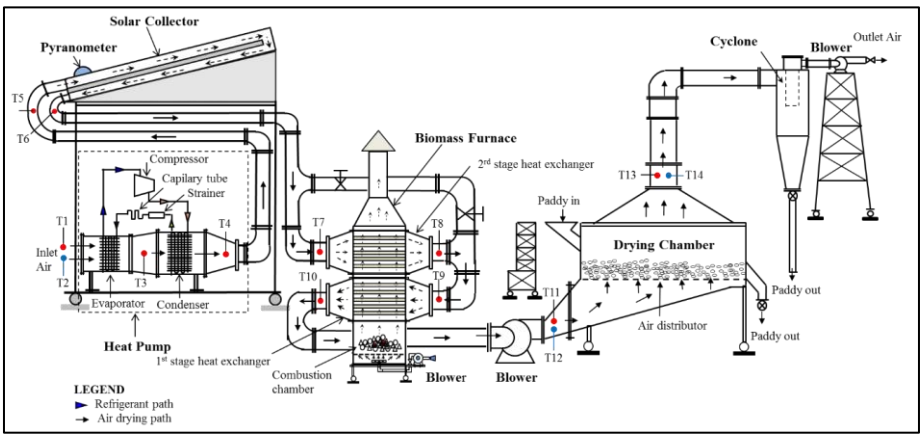

Figure 2. Schematic of an integrated heat pump fluidized-bed dryer incorporating a solar collector and a biomass furnace

An initial MC of 22.19% (wb) was observed in fresh paddy grains (Oryza sativa L.) obtained from Padang, West Sumatra. A total of approximately 12 kg of the grains was then loaded into the drying chamber. The operational conditions of the drying system were comprehensively monitored with several instruments. Air temperatures at various locations within the drying system were measured using thermocouples, whereas solar radiation and airflow rate were measured using a pyranometer and a flowmeter, respectively. The paddy mass change during the drying process was quantified using a electronic balance. Both the paddy mass and air temperatures were recorded periodically at 5 min intervals to accurately monitor the drying dynamics. Coconut-shell charcoal served as the biomass fuel. The relative humidity of the ambient air, as well as the air exiting and entering the drying chamber, was determined from dry- and wet-bulb temperature measurements using a psychrometric chart.

RESULT AND DISCUSSION

The relationship between paddy MC and drying rate as a function of drying time is presented in Figure 3. The paddy MC decreased significantly from 28.52% db (22.19% wb) to 16.28% db (14.0% wb) under operating conditions of 13.78% relative humidity, 70 °C as a mean drying temperature, and 0.1033 kg/s of an air mass flow rate. This MC reduction was achieved within approximately 23.68 minutes of drying. Additionally, Figure 3 shows that the drying rate varied within the range of 0.010 to 0.110 kg/min (averaging 0.042 kg/min). The drying rate was initially high at the early stage of the drying process, corresponding to the high initial MC of the paddy. During paddy drying, the MC gradually decreased, resulting in a continuous reduction in the drying rate over time. This trend indicates that the drying rate is significantly influenced by the paddy MC. Increasing the drying time causes a decrease in the moisture content on a dry basis (%) as well as a decrease in the drying rate (kg/min). These results suggest that the drying process predominantly occurs in the falling-rate period, which is typical for agricultural products such as paddy.

At the initial drying stage (0–5 min), the MC was relatively high, exceeding 28% db, which resulted in the highest drying rate of approximately 0.110 kg/min. This behavior can be attributed to the abundance of free moisture on the paddy surface, allowing rapid evaporation when exposed to hot air. Then, the moisture content decreased steadily from approximately 23% to 17% db as drying time increased to around 10–20 minutes. During this period, the drying rate reduced significantly from about 0.075 kg/min to 0.045 kg/min. Beyond 20 minutes of drying, the moisture content dropped below 16% db, and the drying rate further decreased to values lower than 0.030 kg/min. In this final stage, the drying rate exhibited a gradual and nearly linear reduction. Overall, the data in Figure 3 clearly demonstrate an inverse relationship between moisture content and drying time, accompanied by a decreasing drying rate throughout the process. The absence of a constant-rate drying period suggests that paddy drying under the present operating conditions is dominated by the falling-rate period.

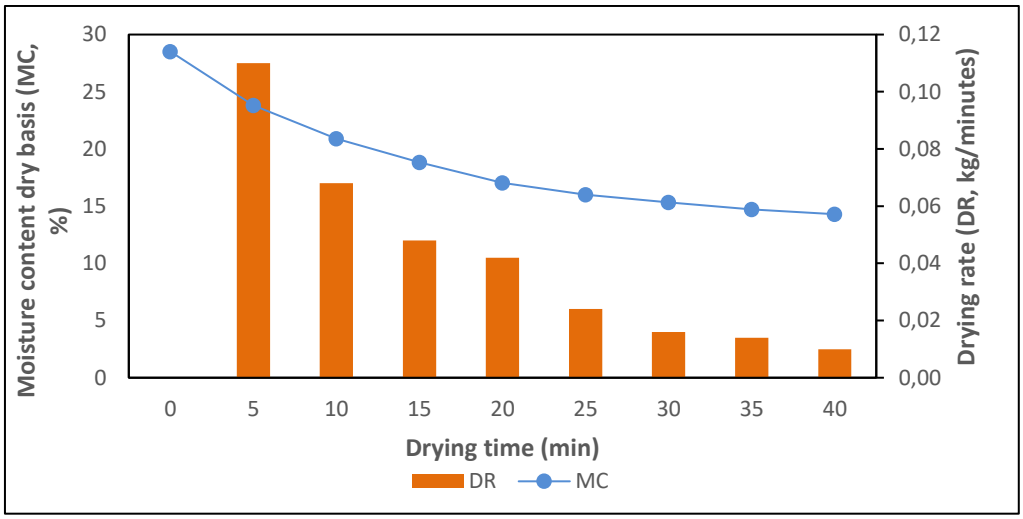

Figure 3. The relationship between drying rate and paddy MC as a function of drying time

The variations in specific energy consumption (SEC), specific thermal energy consumption (STEC), specific moisture extraction rate (SMER), and specific electrical energy consumption (SEEC) as functions of drying time are shown in Figure 4. The results present a decreasing trend in SMER as drying progresses, while SEC, STEC, and SEEC exhibit an opposite increasing tendency. The SMER varied between 0.06 kg/kWh and 0.65 kg/kWh (averaging 0.24 kg/kWh). The SEEC varied between 0.68 kWh/kg and 7.46 kWh/kg (averaging 3.21 kWh/kg), STEC varied between 0.87 and 9.71 kWh/kg (averaging 4.22 kWh/kg), and SEC varied between 1.55 kg/kWh and 17.16 kWh/kg (averaging 7.43 kWh/kg). The results indicate that SMER declined over time, while SEEC, STEC, and SEC increased, due to the gradual decline in the drying rate. Overall, the trends observed in Figure 4 demonstrate that energy efficiency is highest during the initial drying period, then reduces as the drying process approaches lower moisture contents.

At the initial stage of drying (5–10 min), SMER reaches its highest value, exceeding 0.6 kg/kWh, indicating efficient moisture removal with relatively low energy input. During this period, the high moisture content of the paddy facilitates rapid evaporation, resulting in favorable energy utilization. Concurrently, SEC, STEC, and SEEC remain low, reflecting minimal energy demand at the early drying stage. As drying time increases beyond 15 minutes, SMER gradually decreases to values below 0.1 kg/kWh. In contrast, SEC increases steadily from approximately 1 kWh/kg to nearly 18 kWh/kg at 40 minutes, indicating higher energy consumption per unit mass of evaporated moisture. Similarly, STEC and SEEC rise progressively throughout the drying

process. STEC shows a significant increase after 25 minutes, suggesting that thermal energy demand becomes dominant during the last stages of drying. SEEC also shows an increase at a lower rate, reflecting the cumulative electrical energy required for air circulation and system operation.

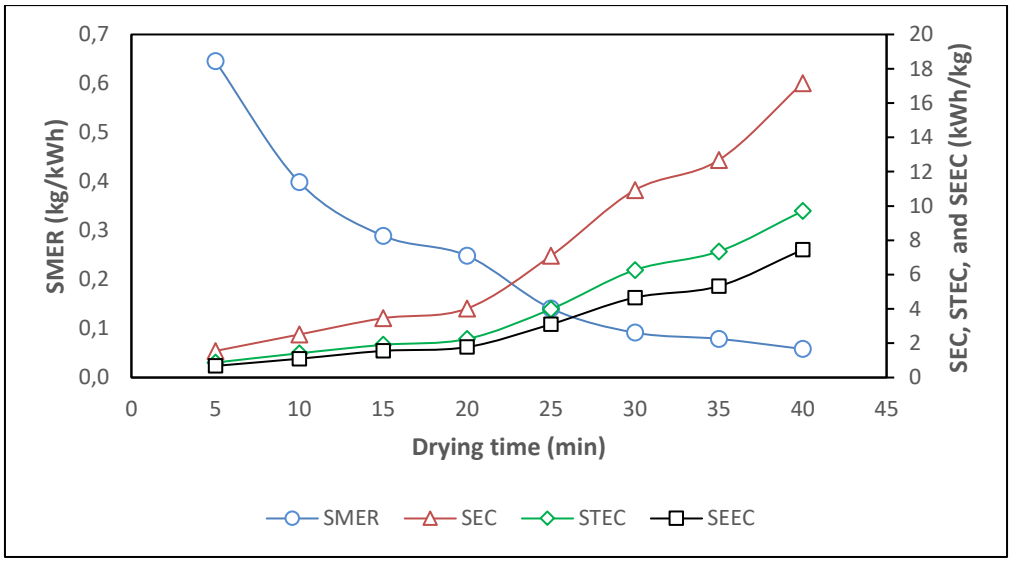

Figure 4. The relationship between SMER, SEEC, STEC, and SEC as a function of drying time

Variations in the thermal efficiencies of the solar collector and biomass furnace at 0.1033 kg/s of the air mass flow rate are illustrated in Figure 5. The solar collector efficiency varied between 24.0% and 39.7% (averaging 31.7%). The biomass furnace exhibited efficiencies from 77.0% to 96.5% (averaging 87.9%). Moreover, Figure 5 illustrates the temporal variations in the coefficient of performance (COP) for the heat pump, as well as the solar collector and biomass furnace thermal efficiencies over the drying process. The results indicate that the heat pump operates with a relatively stable COP throughout the drying period, with values ranging from approximately 2.9 to 3.3 (averaging 3.2), suggesting consistent performance under varying drying conditions. The efficiency of the biomass furnace exhibits significant fluctuations over time, reaching peak values close to 95% around the mid-stage of drying (20-30 min). This behavior can be attributed to more stable combustion conditions and improved heat transfer efficiency as the furnace reaches steady operation. In contrast, the solar collector efficiency shows lower absolute values, varying between approximately 25% and 40%, which reflects the dependence of solar thermal performance on incident solar radiation and thermal losses to the environment. As drying progresses beyond 30 minutes, the biomass furnace and solar collector efficiencies show a slight decline. This decrease is caused by reduced thermal demand as the material decreases in MC, leading to lower useful heat extraction relative to the available energy input. Overall, the trends presented in Figure 5 demonstrate the complementary roles of biomass furnace, solar collector, and heat pump in sustaining stable and efficient drying performance across different stages of the drying process.

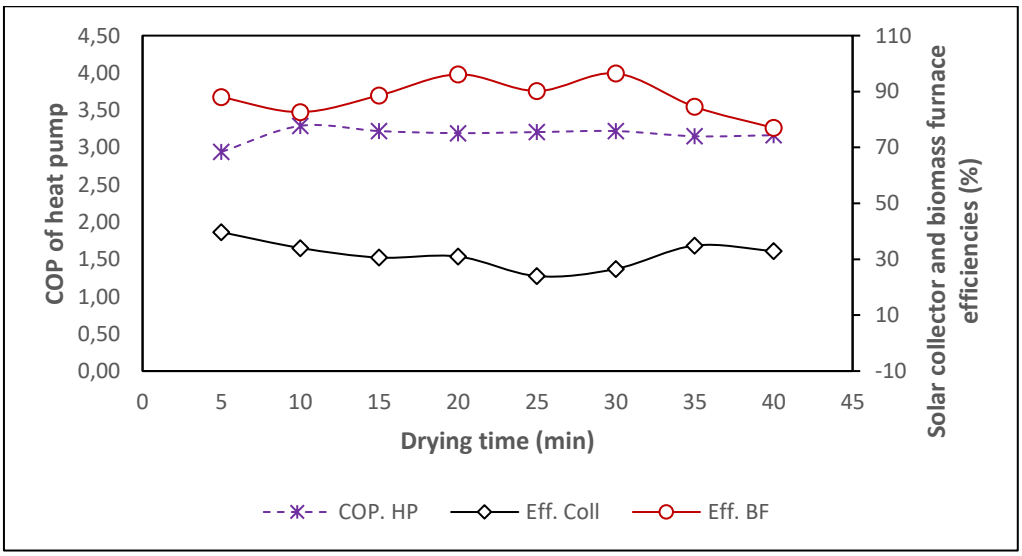

Figure 5. The relationship between the COP of the heat pump, solar collector and biomass furnace efficiencies as a function of drying time

Figure 6 illustrates the heat energy produced by a heat pump, biomass furnace, and solar collector at different drying times. The results show that the biomass furnace consistently provides the highest heat output throughout the drying process, with values ranging from approximately 2.55 kW to 3.19 kW (average 2.91 kW). This indicates that the biomass furnace serves as the primary thermal energy source, supplying stable and sufficient heat in maintaining the drying air temperature. The solar collector produces lower heat energy, ranging from about 0.58 kW to 1.00 kW (averaging 0.79 kW), and exhibits greater fluctuation compared to the other heat sources. These variations can be attributed to changes in solar radiation intensity and ambient conditions during the drying process. Despite its lower contribution, the solar collector plays a complementary role by reducing reliance on biomass fuel and enhancing the total energy efficiency of the hybrid drying system. In contrast, the heat pump condenser contributes a relatively steady heat output, varying between approximately 2.19 kW and 2.45 kW (averaging 2.37 kW). Overall, the combined operation of the heat pump, solar collector, and biomass furnace ensures a balanced and reliable heat supply across different drying stages.

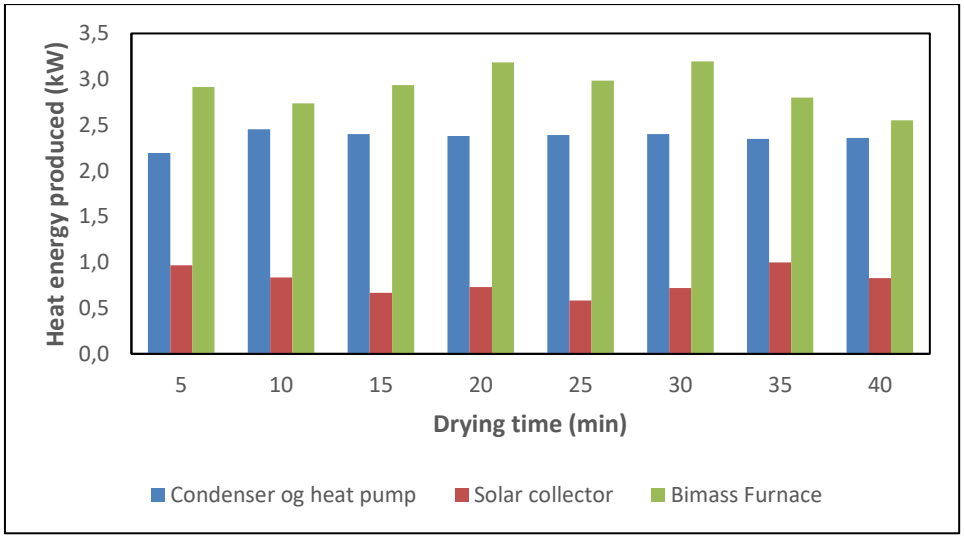

Figure 6. The relationship between heat energy produced and drying time

Figure 7 illustrates the energy fraction of the biomass and solar energy during drying. The fraction of solar energy remains relatively low throughout the drying process, varying between approximately 5.6% and 9.2% (averaging 7.5%). This indicates that solar energy functions primarily as an auxiliary energy source. Minor fluctuations in the solar fraction during drying time are attributed to variations in solar radiation intensity due to solar energy intermittency. Moreover, the biomass energy fraction exhibits consistently higher values, ranging from approximately 24% to 31% (averaging around 27–28%), confirming its dominant contribution to the total energy input. The peak biomass fraction observed at intermediate drying times (15-30 min) suggests increased thermal energy requirements to sustain stable drying temperatures and moisture removal rates. These results indicate that biomass energy plays a critical role in ensuring process continuity and thermal stability, while solar energy contributes to reducing overall biomass consumption and enhancing system energy efficiency.

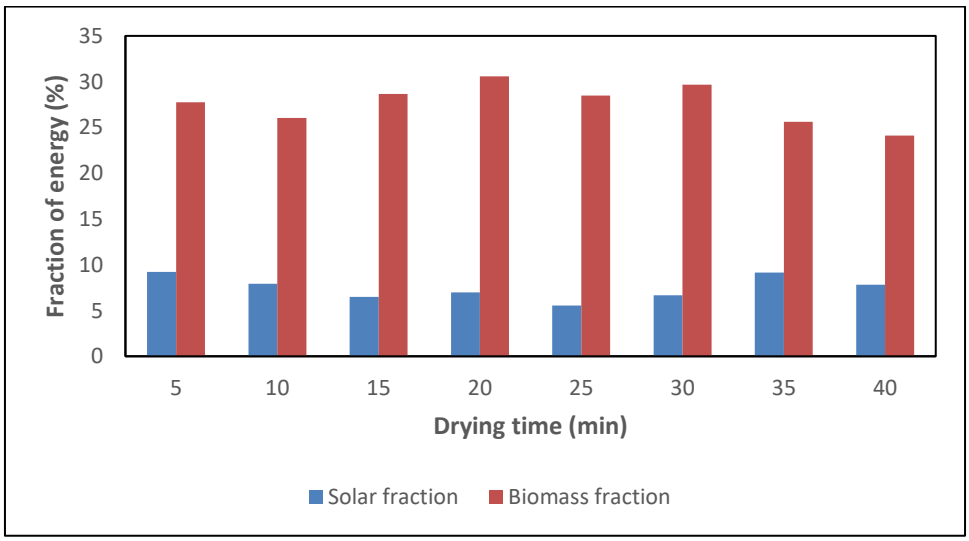

Figure 7. The relationship between energy fraction and drying time

The variation of exergy outflow and inflow, as well as exergy loss over drying is exhibited in Figure 8. The exergy outflow varied between 315.3 J/s and 891.1 J/s, with a mean value of 735.5 J/s, corresponding to the useful exergy carried by the exhaust air and the dried material. In contrast, the exergy inflow varied between 1134.7 J/s and 1456.1 J/s (averaging 1267.8 J/s). The exergy loss, which represents the irreversibility within the system, lay in the range of 373.1 J/s to 902.8 J/s, with an average of 532.4 J/s. The observed fluctuations in exergy parameters with increasing drying time indicate dynamic changes in mass and heat transfer mechanisms within the dryer. Higher exergy losses at certain drying intervals suggest intensified entropy generation due to non-equilibrium heat transfer and pressure losses within the drying chamber.

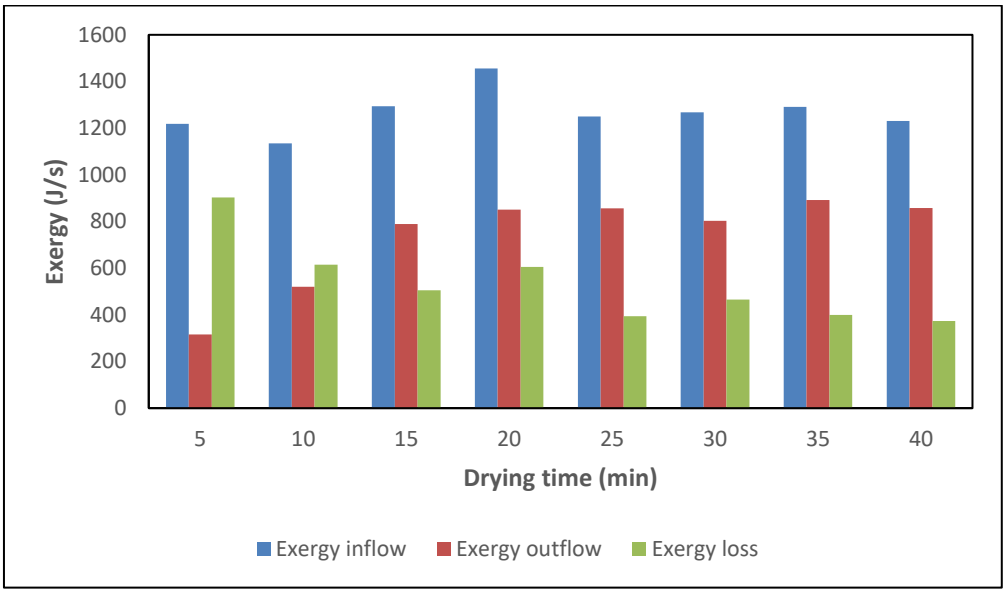

Figure 8. The relationship between exergy variation and drying time

Figure 9 depicts the changes in the thermal and pickup efficiencies of the dryer during the drying process. The thermal efficiencies of the dryer ranged from 3.7% to 40.8% (averaging 21.8%), while the pickup efficiency ranged from 11.4% to 79.5%, with an average value of 40.4%. Figure 9 also shows the variation in exergy efficiency during the drying process, which varied from 25.9% to 69.7%, with an average value of 57.7%. At the initial phase of drying, the thermal and pickup efficiencies were relatively high, but they were reduced toward the end of the process as the drying rate decreased over time.

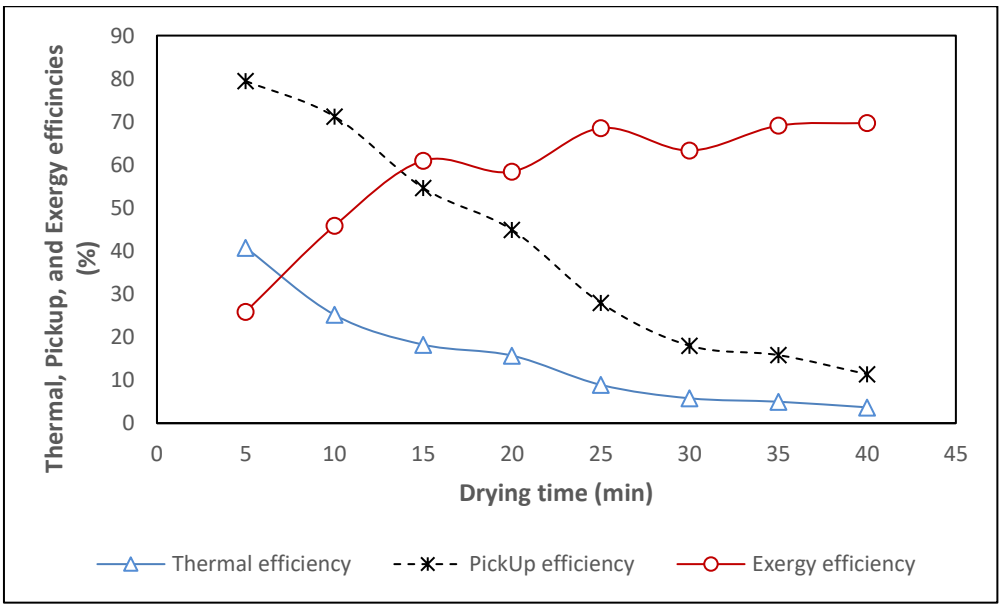

Figure 9. The relationship between thermal, pickup, and exergy efficiencies as a function of drying time

CONCLUSIONS

The paddy drying system combining a heat pump-assisted fluidized-bed dryer incorporating a solar collector and a biomass furnace was tested and assessed. The experiment results indicated that:

1. Paddy moisture content was successfully decreased from 28.52% db to 16.28% db over a period of 23.68 minutes by the drying system, which operated at a mass flow rate of 0.1033 kg/s and 70 °C average temperature.
2. Throughout the process, the drying rate fluctuated between 0.010 kg/min and 0.110 kg/min (averaging 0.042 kg/min).
3. The SMER obtained during the drying process varied between 0.06 kg/kWh and 0.65 kg/kWh (averaging 0.24 kg/kWh).
4. The SEEC, STEC, and SEC exhibited ranges of 0.68 to 7.46 kWh/kg (averaging 3.21 kWh/kg), 0.87 to 9.71 kWh/kg (averaging 4.22 kWh/kg), and 1.55 to 17.16 kWh/kg (averaging 7.43 kWh/kg).
5. The efficiency of the biomass furnace ranged from 77.0% to 96.5% (averaging 87.9%), while solar collector efficiency varied from 24.0% to 39.7% (averaging 31.7%).
6. The COP varied between 2.9 and 3.3, with a mean of 3.2.
7. The heat energy produced varied from 2.19 kW to 2.45 kW (averaging 2.37 kW) for the heat pump condenser, 2.55 kW to 3.19 kW (averaging 2.91 kW) for the biomass furnace, and 0.58 kW to 1.00 kW (averaging 0.79 kW) for the solar collector.
8. The energy fractions obtained in the experiment ranged from 5.6% to 9.2% (averaging 7.5%) for solar fraction and 24.1% to 30.6% (averaging 27.6%) for biomass fraction.
9. The loss of exergy, outflow, and inflow ranged from 373.1 J/s to 902.8 J/s (averaging 532.4 J/s), 315.3 J/s to 891.1 J/s (mean of 735.5 J/s), and 1134.7 J/s to 1456.1 J/s (averaging 1267.8 J/s), respectively.
10. The dryer exhibited thermal efficiencies of 3.7%–40.8% and pickup efficiencies of 11.4%–79.5%, with corresponding mean values of 21.8% and 40.4%.
11. The efficiency of exergy obtained in the experiment ranged from 25.9% to 69.7% (averaging 57.7%).
12. The implementation of a heat recovery exchanger in the drying system results in an approximate 47% decrease in heat energy demand.
13. Heat energy consumption in the drying system was lowered by roughly 47% using a heat recovery exchanger.

REFERENCES

[1] BPS, *Statistik Indonesia*. Jakarta: Badan Pusat Statistik, 2019.

[2] H. K. Purwadaria, "Problems and Priorities of Grain Drying in Indonesia," in *Grain Drying in Asia: Proceeding of an International Conference held at the 74 FAO Regional Office for Asia and the Pacific, ACIAR Proceedings No. 71*, Bangkok, Thailand, 1995, pp. 201–209.

[3] BSN, "Standar Nasional Indonesia Beras Giling," Badan Standardisasi Nasional, Jakarta, 2008.

[4] S. Syahrul, F. Hamdullahpur, and I. Dincer, "Exergy analysis of fluidized bed drying of moist particles," *Exergy, An Int. J.*, vol. 2, no. 2, pp. 87–98, 2002, doi: https://doi.org/10.1016/S1164-0235(01)00044-9.

[5] M. N. Ibrahim, M. S. H. Sarker, N. Ab Aziz, and P. Mohd Salleh, "Drying Performances and Milling Quality of Rice during Industrial Fluidized Bed Drying of Paddy in Malaysia," *Pertanika J. Sci. Technol.*, vol. 23, no. 2, pp. 297–309, 2015.

[6] M. S. H. Sarker, M. N. Ibrahim, N. Abdul Aziz, and M. S. Punan, "Energy and exergy analysis of industrial fluidized bed drying of paddy," *Energy*, vol. 84, pp. 131–138, 2015, doi: https://doi.org/10.1016/j.energy.2015.02.064.

[7] S. Janjai, N. Srisittipokakun, and B. K. Bala, "Experimental and modelling performances of a roof-integrated solar drying system for drying herbs and spices," *Energy*, vol. 33, no. 1, pp. 91–103, 2008, doi: https://doi.org/10.1016/j.energy.2007.08.009.

[8] A. R. Celma and F. Cuadros, "Energy and exergy analyses of OMW solar drying process," *Renew. Energy*, vol. 34, no. 3, pp. 660–666, 2009, doi: https://doi.org/10.1016/j.renene.2008.05.019.

[9] J. Banout, P. Ehl, J. Havlik, B. Lojka, Z. Polesny, and V. Verner, "Design and performance evaluation of a Double-pass solar drier for drying of red chilli (Capsicum annum L.)," *Sol. Energy*, vol. 85, no. 3, pp. 506–515, 2011, doi: https://doi.org/10.1016/j.solener.2010.12.017.

[10] A. Fudholi, K. Sopian, M. A. Alghoul, M. H. Ruslan, and M. Y. Othman, "Performances and improvement potential of solar drying system for palm oil fronds," *Renew. Energy*, vol. 78, pp. 561–565, 2015, doi: https://doi.org/10.1016/j.renene.2015.01.050.

[11] S. Janjai, P. Intawee, J. Kaewkiew, C. Sritus, and V. Khamvongsa, "A large-scale solar greenhouse dryer using polycarbonate cover: Modeling and testing in a tropical environment of Lao People's Democratic Republic," *Renew. Energy*, vol. 36, no. 3, pp. 1053–1062, 2011, doi: https://doi.org/10.1016/j.renene.2010.09.008.

[12] V. Palled, S. R. Desai, Lokesh, and M. Anantachar, "Performance evaluation of solar tunnel dryer for chilly drying," *Karnataka J. Agric. Sci.*, vol. 25, no. 4, pp. 472–474, 2012.

[13] N. Srisittipokakun, K. Kirdsiri, and J. Kaewkhao, "Solar drying of Andrographis paniculata using a parabolicshaped solar tunnel dryer," *Procedia Eng.*, vol. 32, pp. 839–846, 2012, doi: https://doi.org/10.1016/j.proeng.2012.02.021.

[14] J. Prasad and V. K. Vijay, "Experimental studies on drying of Zingiber officinale, Curcuma longa l. and Tinospora cordifolia in solar-biomass hybrid drier," *Renew. Energy*, vol. 30, no. 14, pp. 2097–2109, 2005, doi: https://doi.org/10.1016/j.renene.2005.02.007.

[15] A. Madhlopa and G. Ngwalo, "Solar dryer with thermal storage and biomass-backup heater," *Sol. Energy*, vol. 81, no. 4, pp. 449–462, 2007, doi: https://doi.org/10.1016/j.solener.2006.08.008.

[16] M. A. Leon and S. Kumar, "Design and Performance Evaluation of a Solar-Assisted Biomass Drying System with Thermal Storage," *Dry. Technol.*, vol. 26, no. 7, pp. 936–947, Jul. 2008, doi: https://doi.org/10.1080/07373930802142812.

[17] Hamdani, T. A. Rizal, and Z. Muhammad, "Fabrication and testing of hybrid solar-biomass dryer for drying fish," *Case Stud. Therm. Eng.*, vol. 12, pp. 489–496, 2018, doi: https://doi.org/10.1016/j.csite.2018.06.008.

[18] M. Yahya, "Design and Performance Evaluation of a Solar Assisted Heat Pump Dryer Integrated with Biomass Furnace for Red Chilli," *Int. J. Photoenergy*, vol. 2016, no. 1, p. 8763947, Jan. 2016, doi: https://doi.org/10.1155/2016/8763947.

[19] M. Mohanraj, "Performance of a solar-ambient hybrid source heat pump drier for copra drying under hot-humid weather conditions," *Energy Sustain. Dev.*, vol. 23, pp. 165–169, 2014, doi: https://doi.org/10.1016/j.esd.2014.09.001.

[20] M. Yahya, A. Fudholi, H. Hafizh, and K. Sopian, "Comparison of solar dryer and solar-assisted heat pump dryer for cassava," *Sol. Energy*, vol. 136, pp. 606–613, 2016, doi: https://doi.org/10.1016/j.solener.2016.07.049.

[21] M. Yahya, "Performance Analysis of Solar Assisted Fluidized Bed Dryer Integrated Biomass Furnace with and without Heat Pump for Drying of Paddy," *Int. J. Photoenergy*, vol. 2016, no. 1, p. 3801918, Jan. 2016, doi: https://doi.org/10.1155/2016/3801918.

[22] Y. Qiu, M. Li, R. H. E. Hassanien, Y. Wang, X. Luo, and Q. Yu, "Performance and operation mode analysis of a heat recovery and thermal storage solar-assisted heat pump drying system," *Sol. Energy*, vol. 137, pp. 225–235, 2016, doi: https://doi.org/10.1016/j.solener.2016.08.016.

[23] M. Aktaş, A. Khanlari, B. Aktekeli, and A. Amini, "Analysis of a new drying chamber for heat pump mint leaves dryer," *Int. J. Hydrogen Energy*, vol. 42, no. 28, pp. 18034–18044, 2017, doi: https://doi.org/10.1016/j.ijhydene.2017.03.007.

[24] T. A. Yassen and H. H. Al-Kayiem, "Experimental investigation and evaluation of hybrid solar/thermal dryer combined with supplementary recovery dryer," *Sol. Energy*, vol. 134, pp. 284–293, 2016, doi: https://doi.org/10.1016/j.solener.2016.05.011.

[25] F. Xiang, L. Wang, and X. Yue, "Exergy Analysis and Experimental Study of a Vehicle-Mounted Heat Pump–Assisted Fluidization Drying System Driven by a Diesel Generator," *Dry. Technol.*, vol. 29, no. 11, pp. 1313–1324, Sep. 2011, doi: https://doi.org/10.1080/07373937.2011.592044.